Available online at www.sciencedirect.com
ScienceDirect
Scripta Materialia 64 (2011) 9–12
Scripta MATERIALIA
www.elsevier.com/locate/scriptamat

Toward optimum friction stir welding tool shoulder diameter

A. Arora,[a] A. De[b] and T. DebRoy[a,*]

[a]Department of Materials Science and Engineering, The Pennsylvania State University, University, Park, PA 16802, USA
[b]Department of Mechanical Engineering, Indian Institute of Technology, Bombay, Mumbai 400076, India

Received 3 July 2010; revised 25 August 2010; accepted 26 August 2010
Available online 31 August 2010

Currently friction stir welding tools are designed by trial and error. Here we propose and test a criterion for the design of a tool shoulder diameter based on the principle of maximum utilization of supplied torque for traction. The optimum tool shoulder diameter computed from this principle using a numerical heat transfer and material flow model resulted in best weld metal strength in independent tests and peak temperatures that are well within the commonly encountered range.

Keywords: Friction stir welding; Aluminum alloys; Modeling; High temperature deformation; Tool design

The friction stir welding (FSW) process is now commercially used for the joining of several aluminum alloys [1]. The welding process involves a rotating tool with a shoulder and a pin that generates heat and facilitates the flow of the softened solid alloy behind the tool where the welded joint forms [2]. For the tools to be reused, they must perform reliably under the harsh service conditions of high temperatures and strain rates [3,4]. Since most aluminum alloys are soft, especially at high temperatures, tool erosion and failure are not limiting factors for their welding. In contrast, FSW is yet to be commercially used for hard alloys such as steels and titanium alloys, because of the lack of cost-effective, durable tools that can adequately soften, transport and join these strong alloys repeatedly [3–7].

So far, tools have been designed mostly by trial and error [8]. Most of the previous investigations on the design of tool geometry were focused on optimizing tool pin profiles [8,9]. Tools with cylindrical or tapered pins with or without threads have been designed and widely used [8]. More complex pin profiles, such as a triangular cross-section or a convex external surface, have also been investigated [9]. While the effects of different pin profiles have been studied, very little effort has been made to study the effect of tool shoulder diameter. Since the softening of the material and its flow are both greatly influenced by the shoulder size, the size of the shoulder is a critical factor in tool geometry. Elangovan and Balasubramanian [10] studied the effects of tool shoulder size experimentally and showed that only a tool with a particular shoulder diameter resulted in the highest strength of the joints during FSW of AA6061 alloy. However, the study did not provide any guidelines for the design of tool geometry.

An appropriate design of tool geometry should promote optimum utilization of the available torque. Here we propose and test a criterion for design of tool geometry based on this principle. We use a well-tested three-dimensional heat transfer and material flow model to compute the amount of torque used for both sticking and sliding at the tool–workpiece interface. The proposed criterion is used to identify an optimum shoulder diameter for a given set of welding variables. It is found that the same optimum shoulder diameter results in the best weld joint tensile properties in independent tests, as reported in the literature.

A well-tested three-dimensional heat transfer and visco-plastic flow model for FSW is used for the work. A detailed description of the model is available in the literature [5–7,11–14], so is not repeated here – only its salient features relevant for the present study are discussed briefly. The numerical model solves the momentum conservation equation in a steady state, considering incompressible visco-plastic flow [11–14]. The energy conservation equation considers both the heat generated at the tool–workpiece interface and the volumetric heat generated due to plastic work [11–14]. The rate of heat generated per unit area at the tool–workpiece interface, S, is given by:

$$S = [(1-\delta)\eta\tau + \delta\mu_f P_N](\omega r - U_1 \sin\theta) \quad (1)$$

* Corresponding author. Tel.: +1 814 865 1974; e-mail: debroy@psu.edu

1359-6462/$ - see front matter © 2010 Acta Materialia Inc. Published by Elsevier Ltd. All rights reserved.
doi:10.1016/j.scriptamat.2010.08.052

where ω is tool rotational speed (rad s^{-1}), η is the mechanical efficiency, τ is the shear yield strength, P_N is the axial pressure, δ and μ_f are the spatially variable fractional slip and coefficient of friction respectively, r is the radial distance from the axis of the tool and U_1 is the welding velocity. The first and second terms of Eq. (1) refer to the rate of mechanical and frictional work, respectively, and both of them are converted to heat. The term $(\omega r - U_1 \sin\theta)$ represents the local relative velocity of a point on the tool with the origin fixed at the tool axis. Eq. (1) shows that the shoulder diameter and the tool rotational speed (rpm) are the most influential factors in determining the heat generation rate. It is noteworthy that ωr is much larger than $U_1 \sin\theta$ in Eq. (1) Since the plastic flow behavior and the sticking torque depend on temperature, the shoulder diameter and the rotational speed are the most important factors. Also, the shoulder area is much larger than the pin surface area and, as a result, the pin geometry does not contribute significantly to the torque required for welding. The spatial variations in δ and μ_f in Eq. (1) are derived from the trend of the reported data on total accumulated slip during cross-wedge rolling and are defined as [15]:

$$\delta = 0.31 \times \exp\left(\frac{\omega r}{1.87}\right) - 0.026 \tag{2}$$

$$\mu_f = 0.5 \times exp(-\omega r \times \delta) \tag{3}$$

where ωr is in m s^{-1}. Eqs. (2) and (3) are valid for ωr in the range of 0.1–1.6 m s^{-1}. The volumetric rate of heat generation, S_v, due to plastic deformation is given by:

$$S_v = \lambda \mu \dot{\varepsilon}^2 \tag{4}$$

where μ is the viscosity, $\dot{\varepsilon}$ is the effective strain rate and λ is a constant which represents the fraction of the visco-plastic work that is converted to heat. The spatially variable strain rate $\dot{\varepsilon}$ is computed as follows [11–14]:

$$\dot{\varepsilon} = \sqrt{\frac{2}{3}\left(\left(\frac{\partial u_i}{\partial x_i}\right)^2 + \frac{1}{2}\left(\frac{\partial u_1}{\partial x_2} + \frac{\partial u_2}{\partial x_1}\right)^2 + \frac{1}{2}\left(\frac{\partial u_1}{\partial x_3} + \frac{\partial u_3}{\partial x_1}\right)^2 + \frac{1}{2}\left(\frac{\partial u_3}{\partial x_2} + \frac{\partial u_2}{\partial x_3}\right)^2\right)} \tag{5}$$

where u_i is the velocity component, with $i = 1$, 2 and 3 referring to the three axes in the Cartesian coordinate system. The total torque, M, required during FSW is computed as:

$$\mathrm{M} = \mathrm{M_T} + \mathrm{M_L} \tag{6}$$

where M_T and M_L are the sticking and sliding components of torque, respectively. Hereafter M_T and M_L are referred as sticking torque and sliding torque, respectively, and are computed as follows [11–14]:

$$M_T = \oint_A r_A \times (1 - \delta)\tau \times dA \tag{7}$$

$$M_L = \oint_A r_A \times \delta \mu_f P_N \times dA \tag{8}$$

where r_A is the distance of any infinitesimal area element, dA, from the tool axis. A comparison of Eqs. (7) and (8) with Eq. (1) shows that M_T contributes to the mechanical work that is converted to heat and M_L contributes to frictional heating. The data used for the calculations are presented in Table 1.

Elangovan and Balasubramanian [10] studied FSW of AA6061 with 15, 18 and 21 mm shoulder diameter tools, each with five pin profiles at a constant rotational speed of 1200 rpm and a linear velocity of 1.25 mm s^{-1} for the welding of 6 mm thick plates. They reported that the tool with 18 mm shoulder diameter produced defect-free welds irrespective of pin geometries. Furthermore, the tool with a square pin profile provided superior weld joint tensile properties. However, it is unclear why the 18 mm shoulder diameter resulted in superior welds.

In order to evaluate the effect of shoulder diameter, a well-tested heat transfer and materials flow model is used to compute the temperature and velocity fields, and the torque for several shoulder diameters (12–27 mm) and rotational speeds (900–1500 rpm). The model was able to predict peak temperatures and torques within an error of ± 5% for the FSW of several aluminum alloys, steels and titanium alloys [5–7,11–14]. As expected, the peak temperature increases with shoulder diameter for a given tool rotational speed. As a result, the flow stress of the alloy in the weld region decreases with increase in shoulder diameter. Colegrove and Shercliff [16] used the temperature and flow stress combinations experienced by the material near the tool to evaluate the effects of different pin profiles. They suggested that the flow stress/temperature combination indicated the state of the material that would be useful to understand the design of the tool [16]. In order to examine how the shoulder diameter affects the state of the material, we plotted the computed flow stress and temperature combinations experienced by the materials in Figure 1 for various tool shoulder diameters. In the figure, the darker shades indicate that the specific combination of temperature and flow stress is experienced frequently by many locations within the weld zone. Figure 1 shows that for smaller shoulder diameters the material deforms at low temperatures and high flow stresses, and vice versa. In the hot working literature, a temperature range between 0.8 T_s and T_s, where T_s is the solidus temperature, has been often used [1,2,9,16]. Because of the trend shown in Figure 1, the flow stress vs. temperature plot alone is insufficient to identify an optimal shoulder diameter among the ones considered here.

In order to determine the optimum tool geometry, the two components of the torque are plotted in Figure 2 for various shoulder diameters. As the shoulder diameter increases, the sticking torque, M_T, increases, reaches a maximum and then decreases. This behavior can be examined from Eq. (7), which shows that two main factors affect the value of the sticking torque. First, the strength of the material, τ decreases with increasing temperature due to an increase in the shoulder diameter. Second, the area over which the torque is applied increases with shoulder diameter. As a result, the product of these two components shows the trend indicated in the figure. The sliding torque, M_L, increases continuously with increasing shoulder diameter due to the larger contact area. With the increase in shoulder diameter the total torque increases continuously even when the sticking torque decreases for large shoulder diameters. In this

Table 1. Data used for calculations.

Alloy	AA-6061
Shoulder diameter (mm)	15, 18, 21
Pin diameter (mm)	6
Pin length (mm)	5.5
Pin profile	Cylindrical, no thread
Rotational velocity (rpm)	900, 1200, 1500
Welding speed (mm s^{-1})	1.25
Axial pressure (MPa)	30
Density (kg m^{-3})	2700
*Yield Strength (MPa)	$13.52 + 263.24 \times \left(1 + \exp\left(\frac{T-456.5}{29}\right)\right)^{-1}$
*Specific heat (J kg^{-1} K^{-1})	$9.29 \times 10^{2} - 6.27 \times 10^{-1} T \times 1.48 \times 10^{-3} T^{2} - 4.33 \times 10^{-8} T^{3}$
*Thermal conductivity (W m^{-1} K^{-1})	$2.52 \times 10^{1} \times 3.98 \times 10^{-1} T \times 7.36 \times 10^{-6} T^{2} - 2.52 \times 10^{-7} T^{3}$

* Temperature, T, in K.

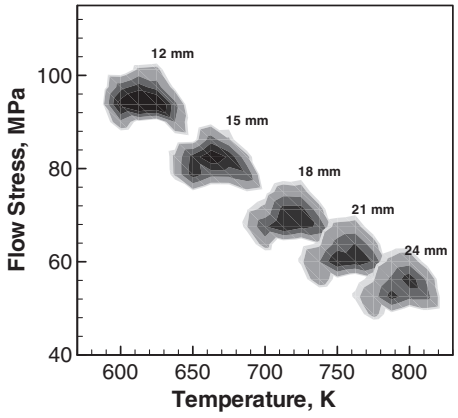

Figure 1. Flow stress and temperature combinations of the weld metal during FSW of AA60601 for various shoulder diameters at 1200 rpm.

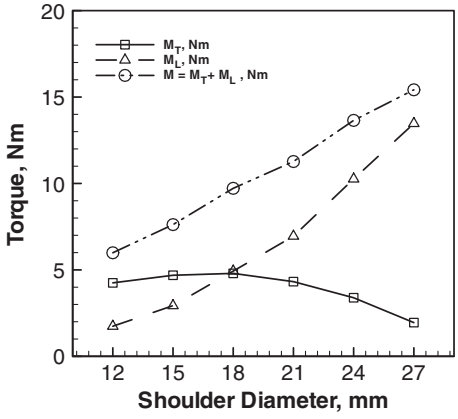

Figure 2. The computed values of sticking, sliding and total torque for various shoulder diameters at 1200 rpm.

regime, the extent of the decrease in the sticking torque is smaller than the increase in the sliding torque. As a result, the total torque increases continuously with shoulder diameter. This behavior is also observed for other tool rotational speeds, as shown in Figure 3. The variation of sticking torque with shoulder diameter can be used to find the optimum tool shoulder diameter, as explained below.

During FSW the tool must have adequate traction on the plasticized material so that material flow occurs

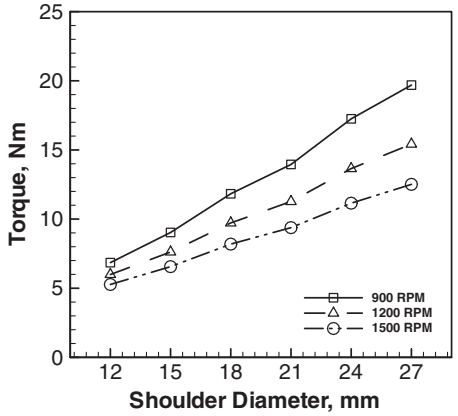

Figure 3. Total torque required during FSW of AA6061 as a function of the tool shoulder diameter for rotational speeds of 900, 1200 and 1500 rpm.

from the leading to the trailing edge of the tool. The shape of the sticking torque vs. shoulder diameter discussed above indicates that the sticking torque is maximum at a certain critical shoulder diameter. Beyond this shoulder diameter, any further increase in torque does not result in improved traction of the tool because of the increase in temperature and the resulting decrease in the flow stress. The sticking torque represents the resistance of the plasticized material against flow around the tool. An optimum amount of material flow around the tool with minimum resistance is needed for a good weld and better tool life in FSW. When the shoulder diameter increases beyond the maximum sticking torque, the material reduces its resistance against flow because of increased temperature and, as a result, the rotating tool loses its ability to influence the movement of the material. Figure 2 indicates that both the sticking and the sliding components of the total torque tend to be equal at a particular shoulder diameter where the sticking torque is maximum. The optimum shoulder diameter corresponds to the maximum value of an objective function, $O(f)$, defined as:

$$O(f) = \left(\frac{M_T}{M_T + M_L} \times \frac{M_L}{M_T + M_L}\right) \tag{9}$$

An optimum tool shoulder diameter should correspond to the criterion when $O(f)$ is closest to its

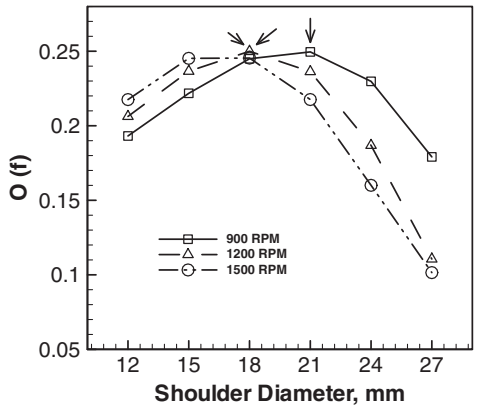

Figure 4. The computed values of the objective function, $O(f)$, as a function of shoulder diameter at tool rotational speeds of 900, 1200 and 1500 rpm.

Table 2. The mechanical properties of welds made using a cylindrical pin profile [10].

Diameter (mm)	Yield strength (MPa)	Ultimate tensile strength (MPa)
15	110.5	131.7
18	130.3	161.7
21	94.0	120.0

maximum possible value (=0.25). Figure 4 shows the variations in the computed values of $O(f)$ as a function of shoulder diameter at three tool rotational speeds. It can be observed that the optimum tool shoulder diameter and rotational speed combinations are (21, 900), (18, 1200) and (18, 1500) for the range of welding parameters considered in the present study. Elangovan and Balasubramanian [10] have also reported that the tool with an 18 mm shoulder diameter provided the best weld joint strength at a rotational speed of 1200 rpm, as shown in Table 2. This shoulder diameter is three times the plate thickness. The shoulder diameter most commonly used in industry is about 2.5–3 times the thickness of the aluminum alloy plates [17]. The computed peak temperatures for the optimized shoulder diameters were in the range of $0.87–0.90T_s$. This temperature range is well within the range of peak temperature commonly used in the FSW of AA6061.

A three-dimensional heat transfer and visco-plastic flow model is used to develop a criterion to identify the optimum tool shoulder diameter for the FSW of AA6061. The criterion calls for an equal partitioning of the supplied torque between sticking and sliding to identify the optimum tool shoulder diameter. The optimum shoulder diameters were determined for rotational speeds of 900, 1200 and 1500 rpm. The optimum shoulder diameter of 18 mm at 1200 rpm has resulted in superior tensile properties in independent tests, as reported in the literature. The computed peak temperatures for all three optimized shoulder diameters were in the range of peak temperatures commonly encountered in the FSW of AA6061.

The authors thank Dr. Thomas J. Lienert of Los Alamos National Laboratory for helpful comments in the preparation of this manuscript. This research was supported by a grant from the Materials Division, Office of Naval Research, Dr. William Mullins, Contract Monitor.

[1] P.R. Nandan, T. DebRoy, H.K.D.H. Bhadeshia, Prog. Mater. Sci. 53 (2008) 980.
[2] W. M. Thomas, E. D. Nicholas, J. C. Needham, M. G. Murch, P. Templesmith, C. J. Dawes, Int. Patent Appl. No. PCT/GB92/02203 and GB Patent Appl. No. 9125978.8, Dec.1991, U.S. Patent Appl. No. 5460317, Oct.1995.
[3] H.K.D.H. Bhadeshia, T. DebRoy, Sci. Technol. Weld. Joining 14 (2009) 193.
[4] T. DebRoy, H.K.D.H. Bhadeshia, Sci. Technol. Weld. Joining 15 (2010) 266.
[5] R. Nandan, G.G. Roy, T.J. Lienert, T. DebRoy, Sci. Technol. Weld. Joining 11 (2006) 526.
[6] R. Nandan, G.G. Roy, T.J. Lienert, T. DebRoy, Acta Mater. 55 (2007) 883.
[7] R. Nandan, T.J. Lienert, T. DebRoy, Int. J. Mater. Res. 99 (2008) 434.
[8] W.M. Thomas, K.I. Johnson, C.S. Wiesner, Adv. Eng. Mater. 5 (2003) 485.
[9] P.A. Colegrove, H.R. Shercliff, Sci. Technol. Weld. Joining 9 (2004) 352.
[10] K. Elangovan, V. Balasubramanian, Mater. Des. 29 (2008) 362.
[11] R. Nandan, G.G. Roy, T. DebRoy, Metall. Mater. Trans. A 37A (2006) 1247.
[12] R. Nandan, B. Prabu, A. De, T. DebRoy, Weld. J. 86 (2007) 313s.
[13] A. Arora, R. Nandan, A.P. Reynolds, Scr. Mater. 60 (2009) 13.
[14] A. Arora, Z. Zhang, A. De, T. DebRoy, Scr. Mater. 61 (2009) 863.
[15] Q. Li, M. Lovell, J. Mater. Process. Technol. 160 (2005) 245.
[16] P.A. Colegrove, H.R. Shercliff, Sci. Technol. Weld. Joining 11 (2006) 429.
[17] T. J. Lienert, private communication, June 2010.